


# Exciton and valley dynamics in $WSe_2$/GaAs heterostructure

Xin Wei(魏鑫), Yuanhe Li(李元和), Wenkai Zhu(朱文凯), Rongkun Han(韩荣坤), Jianhua Zhao(赵建华), Kaiyou Wang(王开友), and Xinhui Zhang(张新惠)

**Citatio:**Chin. Phys. B, 2025, 34 (**9**): 096701. DOI: 10.1088/1674-1056/add504
http://cpb.iphy.ac.cn; http://iopscience.iop.org/cpb

**What follows is a list of articles you may be interested in**

---

## Shear viscosity of an ultracold Fermi gas in the BCS-BEC crossover

Jing Min(闵靖), Xiangchuan Yan(严祥传), Da-Li Sun(孙大立), Lu Wang(王璐), Xin Xie(谢馨), Xizhi Wu(吴熙至), Shi-Guo Peng(彭世国), and Kaijun Jiang(江开军)

Chin. Phys. B, 2025, 34 (**5**): 053103. DOI: 10.1088/1674-1056/adc403

## Effect of conical intersection of benzene on non-adiabatic dynamics

Duo-Duo Li(李多多) and Song Zhang(张嵩)

Chin. Phys. B, 2022, 31 (**8**): 083103. DOI: 10.1088/1674-1056/ac5607

## Liquid phase epitaxy magnetic garnet films and their applications

Yi-Heng Rao(饶毅恒), Huai-Wu Zhang(张怀武), Qing-Hui Yang(杨青慧), Dai-Nan Zhang(张岱南), Li-Chuan Jin(金立川), Bo Ma(马博), Yu-Juan Wu(吴玉娟)

Chin. Phys. B, 2018, 27 (**8**): 086701. DOI: 10.1088/1674-1056/27/8/086701

## Spin detection and manipulation with scanning tunneling microscopy

Chunlei Gao(高春雷)

Chin. Phys. B, 2018, 27 (**10**): 106701. DOI: 10.1088/1674-1056/27/10/106701

## Effects of pressure and gas-jet thickness on the generation of attosecond pulse

Li Xiao-Yong (李小勇), Wang Guo-Li (王国利), Zhou Xiao-Xin (周效信)

Chin. Phys. B, 2014, 23 (**1**): 013102. DOI: 10.1088/1674-1056/23/1/013102

---

**SPECIAL TOPIC — Exciton physics: Fundamentals, materials and devices**

# Exciton and valley dynamics in $WSe_2$/GaAs heterostructure

Xin Wei(魏鑫)[1,2], Yuanhe Li(李元和)[1,2], Wenkai Zhu(朱文凯)[1,2], Rongkun Han(韩荣坤)[1,2], Jianhua Zhao(赵建华)[1,3], Kaiyou Wang(王开友)[1,2], and Xinhui Zhang(张新惠)[1,2,†]

[1] *State Key Laboratory of Semiconductor Physics and Chip Technologies, Institute of Semiconductors, Chinese Academy of Sciences, Beijing* 100083, *China*

[2] *Center of Materials Science and Optoelectronics Engineering, University of Chinese Academy of Sciences, Beijing* 100049, *China*

[3] *National Key Laboratory of Spintronics, Hangzhou International Innovation Institute, Beihang University, Hangzhou* 311115, *China*

(Received 20 March 2025; revised manuscript received 25 April 2025; accepted manuscript online 7 May 2025)

Transition metal dichalcogenide (TMDC) monolayers provide an ideal platform for exciton and valley-spintronics exploration due to their unique properties. Integrating TMDC monolayers with conventional semiconductors allows for harnessing the unique properties of both materials. This strategy holds great promise for the development of advanced optoelectronics and spintronic devices. In this work, we investigated exciton and valley dynamics in $WSe_2$/GaAs heterostructure by employing the femtosecond pump–probe ultrafast spectroscopy. Facilitated by the charge transfer within the heterostructure, it was found that the exciton of $WSe_2$ exhibited much longer lifetime of nanosecond than that of the $WSe_2$ monolayer counterpart. Especially, a significantly long valley lifetime up to $\sim 2.7$ ns was observed for trions of $WSe_2$ in the heterostructure even under the off-resonant excitation, which is found to be associated with the resident electrons accumulated at the interface resulting from the charge transfer and resultant interfacial electric field. Our results provide fundamental references for conventional semiconductor-integrated TMDC heterostructures that have great potential for designing novel optoelectronic and spintronic devices.

**Keywords:** transition metal dichalcogenide (TMDC) heterostructure, exciton, dynamics, charge transfer, femtosecond time-resolved spectroscopy

**PACS:** 67.30.hj, 31.70.Hq, 72.25.Rb, 78.55.–m

**DOI:** 10.1088/1674-1056/add504 **CSTR:** 32038.14.CPB.add504

## 1. Introduction

Transition metal dichalcogenides (TMDCs) have emerged as a candidate for building optoelectronic and spintronic devices in the last decade.[1–3] The monolayer TMDCs usually possess direct band gaps in the visible-infrared range and strong spin–orbit coupling, which enable strong optical absorption and exotic exciton properties.[4,5] In the monolayer TMDCs, the two inequivalent valleys are located at the corners of the hexagonal Brillouin zone, and the unique valley-contrasting characteristics allow direct manipulation of the valley states by external optical, electric, and magnetic fields.[6–10] In addition, TMDC heterostructures have also attracted intense research interest for their novel optoelectronic properties arising from the charge transfer and interlayer coupling.[3,11,12] Coupling between TMDC and substrates can affect the screening of charge carriers, leading to modifications in carrier mobility and transport properties.[13–15] Among the studied TMDC heterostructures, the heterostructures combining monolayer TMDCs with traditional bulk semiconductors such as $MoS_2$/GaAs, $WS_2$/GaAs, $WSe_2$/GaN, $MoS_2$/Ge, and $MoS_2$/ZnS, in which the band alignment is suggested to be type II, bring some advantages over the mature three-dimensional (3D) semiconductors while retaining novel properties of two-dimensional (2D) TMDCs.[16–20] Though there have been intense studies on the 2D/2D TMDC heterostructures,[3,21,22] investigations of the exciton and charge transfer dynamics in 2D/3D TMDC heterostructures are very limited. Gallium arsenide (GaAs) is a direct bandgap semiconductor widely used in microelectronics and optoelectronics,[23] with reasonably long carrier and spin lifetimes up to nanosecond timescale for optimally doped n-type GaAs.[24,25] The exciton and valley dynamics of TMDCs are expected to be greatly influenced by the charge transfer process when forming heterostructures with GaAs, however, this issue has not been systematically investigated so far. It is thus important to unveil the exciton and valley dynamics for GaAs-based TMDC heterostructures, which is fundamentally important for the performance of large-scale optoelectronic and spintronic devices made from TMDC/GaAs heterostructures.

In this work, by employing the degenerate and non-degenerate pump–probe transient reflectivity (TRR, $\Delta R/R$) and Kerr rotation (TRKR, $\Delta\theta/\theta$) techniques, we explored the exciton and valley depolarization dynamics of the $WSe_2$/GaAs heterostructure. The exciton of $WSe_2$ in the heterostructure

†Corresponding author. E-mail: xinhuiz@semi.ac.cn

© 2025 Chinese Physical Society and IOP Publishing Ltd. All rights, including for text and data mining, AI training, and similar technologies, are reserved.

was found to survive much longer than that in the monolayer $WSe_2$ counterpart under resonant pump and probe, which was attributed to the non-radiative scattering processes and reduced exciton–exciton annihilation owing to the charge transfer. The trions of $WSe_2$ in the heterostructure exhibit significantly long valley lifetime up to 2.7 ns even under the off-resonant excitation. This long valley lifetime of trions was believed to be associated with the resident electrons trapped at the interface by the charge-transfer induced electric field, as well as the reduced intervalley electron–hole exchange interactions. In addition, the carrier lifetime of GaAs in the heterostructure was prolonged compared to the GaAs substrate owing to the reduced electron–hole recombination as a result of interfacial charge transfer. The experimental findings suggest the $WSe_2$/GaAs heterostructure as a promising candidate for novel optoelectronic and spintronic applications.

## 2. Experimental details

A n-type doped GaAs sample was first prepared via molecular beam epitaxy (MBE) technique by adopting the structure design proposed for efficient spin injection.[26,27] A 500 nm GaAs buffer layer with a n-type doping concentration of $5\times10^{16}$ cm$^{-3}$ was first grown on a semi-insulating GaAs (001) substrate, followed by depositing a 15 nm n-doped GaAs layer with a gradient doping concentration of $5\times10^{16}$–$5\times10^{18}$ cm$^{-3}$. Then a 5 nm-thick n-type GaAs layer with a doping concentration of $5\times10^{18}$ cm$^{-3}$ was deposited on the top. The MBE-grown GaAs sample was then passivated using standard ammonium sulfide solution for 5 min to reduce surface state density.[28] The $WSe_2$ monolayer was mechanically exfoliated onto a 285 nm-thick $SiO_2$/Si substrate and then covered with h-BN flake for protection. The h-BN/$WSe_2$ stack was subsequently transferred onto the passivated GaAs substrate with the assistance of polycarbonate film. Another $WSe_2$ reference sample was exfoliated on $SiO_2$/Si from the same bulk material and covered with h-BN flake. The fabricated $WSe_2$/GaAs heterostructure and its band alignment were displayed in Fig. 1, in which the type-II band alignment was illustrated as has been proved in previous studies.[29,30]

The steady-state photoluminescence (PL) under the excitation of a continuous-wave laser at 632 nm was collected by a micro-PL setup with Horiba Jobin Yvon iHR550 spectrometer equipped with a Si CCD. The circularly-polarized PL was detected by combining a quarter wave plate and a Glan–Taylor prism at the entrance of the spectrometer, under the circularly-polarized excitation. The degree of PL circular polarization is determined by $P_c = (I_+ - I_-)/(I_+ + I_-)$, where $I_+$ and $I_-$ correspond to the $\sigma^+$ and $\sigma^-$ components of the detected PL intensity, respectively. The TRR and TRKR experiments were conducted by using a wavelength-tunable femtosecond Ti:sapphire laser system (Chameleon Ultra II, Coherent, Inc.) comprising an optical parameter oscillator (OPO), with a pulse width of 150 fs and repetition rate of 80 MHz. The photon energy of pump and probe beams can be further chosen from a supercontinuum white light output from a nonlinear photonic crystal fiber (FemotoWHITE-800, NKT Photonics) under excitation of the Ti:sapphire laser. The reflected probe beam was detected by a silicon detector for $\Delta R/R$, and a balanced Si detector for $\Delta\theta/\theta$ measurements. With an Olympus 50× objective lens, the focused beam diameter on the sample is $\sim 2$ μm for all measurements.

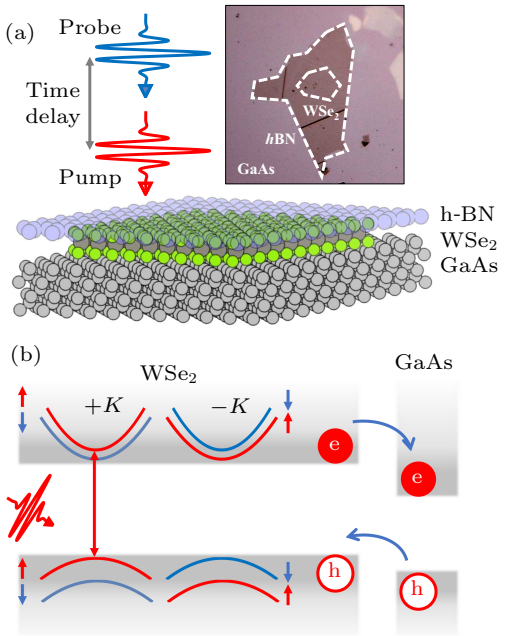



**Fig. 1.** (a) Schematic structure and an optical microscopy image of the prepared $WSe_2$/GaAs heterostructure protected by h-BN flake. (b) Band alignment and schematic charge transfer process in $WSe_2$/GaAs heterostructure upon optical excitation.

## 3. Results and discussion

The PL of $WSe_2$/GaAs and $WSe_2$/$SiO_2$ was first measured at $T = 10$ K, as shown in Fig. 2(a). The PL peaks at 719 nm (1.7246 eV) and 730.7 nm (1.6970 eV) for $WSe_2$/$SiO_2$ correspond to the neutral exciton and trions, as previously reported.[31] The energy difference between the neutral exciton and trions is 27.6 meV, indicating a n-type doping of the studied $WSe_2$.[32–34] The PL responses of $WSe_2$/GaAs showed that both the neutral exciton (706.6 nm, 1.7549 eV) and trions (720 nm, 1.7222 eV) peaks are blue-shifted (30.3 meV for trions and 25.2 meV for neutral excitons) comparing to that of $WSe_2$/$SiO_2$, since the dielectric environment has changed.[35,36] Given the energy difference of 32.7 meV between the neutral exciton and trions PL peaks for $WSe_2$/GaAs, $WSe_2$ remains n-type after transfer on top of GaAs. Apart from the blue-shifts for the PL energy peaks, relative intensity of the neutral exciton and trions at $T = 10$ K in $WSe_2$/GaAs has changed compared to that in $WSe_2$/$SiO_2$ due to different carrier concentration. Moreover, one can observe additional

two weak PL peaks denoted with $X_1$ and $X_3$ besides a relatively strong peak $X_2$ that also appears in $WSe_2/SiO_2$. These PL responses are defect-associated peaks, and are further confirmed by the temperature and excitation power dependent PL measurements. The temperature dependent PL results in Fig. 2(b) show that the peak positions of $X_1$, $X_2$ and $X_3$ do not change with temperature and become absent when rising temperature above 50 K. Moreover, our excitation power dependent PL results (not shown here) also show a sublinear dependence of the integrated PL intensity ($I$) of $X_1$, $X_2$ and $X_3$ with the excitation power density ($P$), with $k$ extracted to be about 0.80, 0.77 and 0.73 for $X_1$, $X_2$ and $X_3$ peaks by evaluating the power law $I = P^k$. Since peak $X_2$ appears in both samples, while $X_1$ and $X_3$ only exist in $WSe_2/GaAs$, the above results suggest that peak $X_2$ is associated with an intrinsic defect that exists in the bulk crystal $WSe_2$ used in this work, and peaks $X_1$ and $X_3$ should be related to the interfacial defects induced during heterostructure fabrication. As previously reported,[35,37] the enhanced dielectric disorder within the heterostructure would cause increased defects and localized states. Usually, for the monolayer $WSe_2$ on $SiO_2/Si$, the strong PL response of trions at low temperature would decrease as temperature rises, and eventually diminishes above $\sim$ 120 K. However, for the $WSe_2/GaAs$ heterostructure investigated in this work, one can notice a stronger PL response of trions when temperature rises to 50 K, accompanied by the PL quench of defects-associated

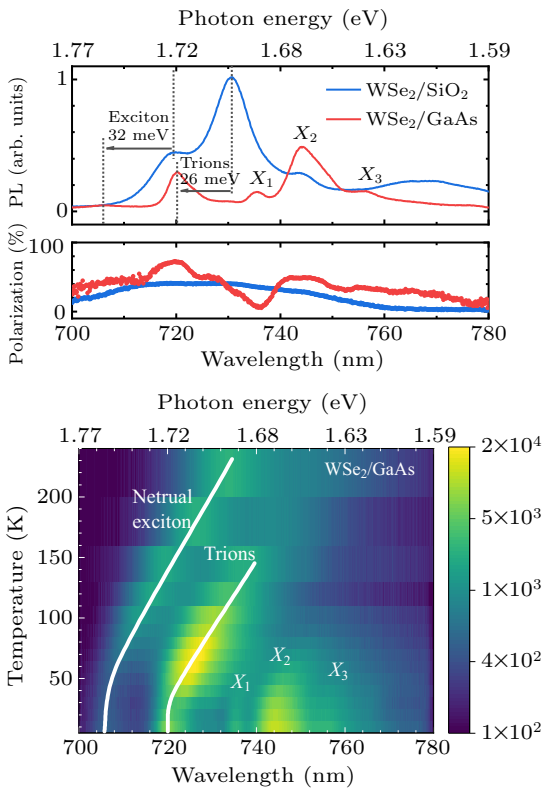



**Fig. 2.** (a) PL spectra of the $WSe_2/GaAs$ and $WSe_2/SiO_2$ (upper panel), as well as the deduced circular polarization degree (lower panel) for both samples measured at temperature of 10 K. (b) Temperature-dependent PL intensity contour plot of $WSe_2/GaAs$ (logarithmic coordinate).

$X_1$, $X_2$ and $X_3$ peaks as shown in Fig. 2(b). Even though there exist additional defects in $WSe_2/GaAs$ heterostructure, one can see in the lower panel of Fig. 2(a) that the circular polarization degree of trions can still reach up to 70% at $T = 10$ K in $WSe_2/GaAs$, which is higher than that of reference $WSe_2/SiO_2$ (maximum only 40%). It is expected that, higher circular polarization degree of trions can be obtained by improving the interface quality and optimizing the doping concentration of $WSe_2$ and GaAs, and could be further modulated with help of external bias control.

To further investigate the lifetimes of neutral exciton and trions as well as the charge dynamics in $WSe_2/GaAs$ heterostructure, we then carried out the TRR and TRKR measurements. We first performed degenerate pump–probe measurements with the same pump and probe photon energies in resonance with that of neutral excitons and trions, respectively, for both $WSe_2/GaAs$ heterostructure and the reference $WSe_2$ at a low temperature of 10 K. The exciton-bound electron and hole can radiatively and non-radiatively recombine to give rise to multi-exponential decay dynamics. By fitting the raw data presented in Fig. 3 with a bi-exponential decay function, the extracted lifetimes of neutral exciton for $WSe_2/GaAs$ are $\sim$ 99 ps ($\tau_1$) and $\sim$ 1.9 ns ($\tau_2$), which are significantly prolonged compared with $\sim$ 38 ps ($\tau_1$) and $\sim$ 0.9 ns ($\tau_2$) obtained for $WSe_2$ reference sample. The short-lived decay component ($\tau_1$) of neutral exciton is mainly related to the direct radiative recombination process, exciton–exciton annihilation, bright–dark exciton scattering, and defect-assisted recombination in $WSe_2$,[31,38] whereas the long-lived decay component ($\tau_2$) was suggested to be associated with the dark exciton decay.[39] Rafael *et al.* recently reported the charge dynamics of a $WSe_2/GaAs$ heterostructure.[29] They yielded similar long carrier lifetime up to 3.5 ns, which was suggested to be associated with the non-radiative scattering processes as a result of lacking available states at $WSe_2$ band edges. The PL intensity of neutral exciton in the heterostructure is far lower than that of the reference sample as shown in Fig. 2(a), indicating that the exciton density in $WSe_2/GaAs$ heterostructure is lower than that of the reference sample owing to the dissociation of excitons and the resultant diminished available states at the band edge of $WSe_2$ as suggested in Ref. [29]. This reduced PL intensity of neutral exciton in $WSe_2/GaAs$ can be a direct consequence of charge transfer within the type-II heterostructure as illustrated in Fig. 1(b). As a result of dissociation of excitons in $WSe_2$ facilitated by the charge transfer, the prolonged neutral exciton lifetime up to 1.9 ns in $WSe_2/GaAs$ heterostructure is attributed to the reduced non-radiative scattering and exciton–exciton annihilation effect whose strength is proportional to the exciton concentration,[40] while the short-lived decay components $\tau_1$ within tens of ps for neutral exciton in both samples are dominated by the direct radiative recom-

bination process.[38,41–44] However, for the lifetime of trions, the results presented in Fig. 3 show that there is no significant difference between the two samples. Considering the dense interfacial defects existing in the $WSe_2$/GaAs heterostructure as revealed in the PL responses in Fig. 2, and the fact that the shorter lifetime $\tau_1$ was slightly reduced from $\sim$ 15 ps for the reference $WSe_2$ to $\sim$ 2 ps for $WSe_2$/GaAs, this short-lived decay component ($\tau_1$) for trions was suggested to relate to the defect-assisted nonradiative recombination process, while the long-lived decay component ($\tau_2$) is associated with the radiative recombination.[38,41–44] As previously demonstrated by Wang *et al.*,[43] the carrier capture via Auger scattering and defect-assisted nonradiative recombination can play a crucial role in the carrier and exciton relaxation. This may also be the reason for the observed similar lifetime of trions for the two samples, since trions are located closer to the defect states and the negatively charged trions could facilitate Auger scattering and the resulting defect-assisted non-radiative recombination. Another tentative explanation is that the negatively charged trions could experience Coulomb scattering via accumulated charges and electric dipoles at the interface owing to the charge transfer, as will be discussed later. These nonradiative recombination processes can dominate the decay of trions, so that the lifetime of trions does not change much comparing the two samples.

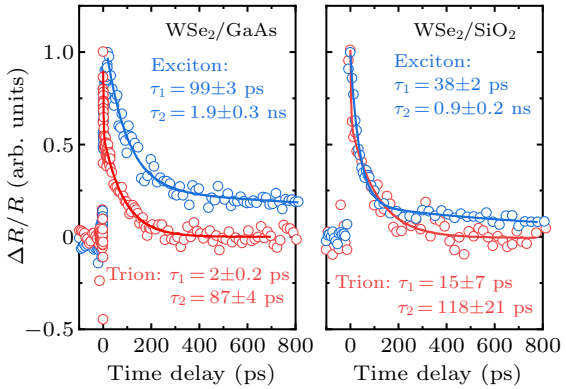



**Fig. 3.** The degenerate TRR ($\Delta R/R$) results of the two samples with the pump and probe photon energies tuned to be resonant with those of neutral exciton and trions for both samples. Dots represent experimental data, and lines are fitting results.

We then performed the two-color TRR and TRKR measurements by tuning the pump photon energy at 1.8 eV and probe photon energies in resonance with those of neutral excitons and trions at $T = 6$ K, respectively, for both the reference $WSe_2$ and $WSe_2$/GaAs heterostructure, as presented in Figs. 4(a) and 4(b). The long lifetime $\tau_2$ for the neutral exciton and trions by the $\Delta R/R$ measurements are determined to be only $\sim$ 400 ps and $\sim$ 34 ps for $WSe_2$/$SiO_2$, respectively, which are shorter than that obtained under resonant pump–probe as shown in Fig. 3. This is because the momentum scattering under off-resonant excitation is greatly enhanced. The valley polarization lifetime for both the exciton and trions evaluated by the $\Delta\theta/\theta$ measurements is only 1.5–2.0 ps for the reference $WSe_2$, which is on a similar timescale to previous reports for monolayer $WSe_2$.[10,31,45–47] The dominant mechanism responsible for the rapid valley depolarization in $WSe_2$ was ascribed to the intervalley electron–hole exchange interaction.[48,49] In contrast to $WSe_2$/$SiO_2$, for the $WSe_2$/GaAs heterostructure as presented in Fig. 4(b), the time evolution of valley depolarization for the exciton and trions by the $\Delta\theta/\theta$ measurements nearly resembles the relaxation processes of neutral exciton and trions measured by $\Delta R/R$. The evaluated lifetimes for the exciton and trions by $\Delta R/R$ are $\sim$ 109 ps and $\sim$ 900 ps, and the characteristic decay times for valley depolarization of exciton and trions are in the time scale of $\sim$ 77 ps and $\sim$ 600 ps, respectively. It is worth noting that the valley lifetime of trions in $WSe_2$/GaAs ($\sim$ 600 ps) has been significantly prolonged by two orders of magnitude compared to that in $WSe_2$/$SiO_2$ ($\sim$ 1.5 ps). Especially, as shown in Fig. 4(c), the longer valley lifetime of trions up to $\sim$ 2.7 ns for $WSe_2$/GaAs heterojunction was observed when fine tuning the probe photon energy to be 1.73 eV, which is at the high-energy tail for trions PL peak of $WSe_2$. The distinct valley depolarization difference of the two samples suggests the emergence of new valley relaxation channels in $WSe_2$/GaAs, likely linked to the charge transfer process. Therefore, we tuned the pump photon energy to further unveil the influence of charge transfer on the valley relaxation process as below. It needs to be emphasized that, previously reported valley lifetime of trions up to nanosecond for monolayer $WSe_2$ on $SiO_2$/Si could only be observed by fine tuning pumping photon energy to be nearly resonant with trions.[9,48,50,51] While for the $WSe_2$/GaAs heterojunction investigated here, the valley depolarization lifetime as long as $\sim$ 2.7 ns for trions was observed under off-resonant excitation condition (1.80 eV). This long valley lifetime of trions is suspected to result from the Rashba spin splitting in $WSe_2$ and resident electrons accumulated at the interface caused by the interfacial electric field in $WSe_2$/GaAs heterojunction. Cheng *et al.* reported large Rashba spin splitting in monolayer TMDCs induced by a perpendicular electric field using first principles.[52] They predicted a nonlinear Rashba spin splitting as large as $\sim$ 15.7 meV in monolayer $WSe_2$, arising from the electric field-induced out-of-plane mirror symmetry breaking. For the $WSe_2$/GaAs heterojunction, the charge transfer is expected to accumulate charges at the interface, creating electric dipoles and a resultant interfacial electric field.[30] Previous study on $WSe_2$/GaN heterostructure also verified the existence of trions composed of electron–hole pairs in $WSe_2$ and electrons accumulated at the interface.[16] In addition, it should be noted that, since the spin split-off band of GaAs is also excited under pumping at 1.8 eV, holes transferred from GaAs to $WSe_2$ are unpolarized, which can reduce

the valley polarization degree of neutral exction and trions in $WSe_2$. Thus, the valley polarization in $WSe_2$ is mostly dependent on the electrons. The above discussions suggest that the long valley lifetime of trions observed in $WSe_2$/GaAs heterojunction under optimal optical probe condition originates from the resident electrons accumulated at the interface, as well as the reduced electron–hole exchange interaction owing to the Rashba spin splitting.

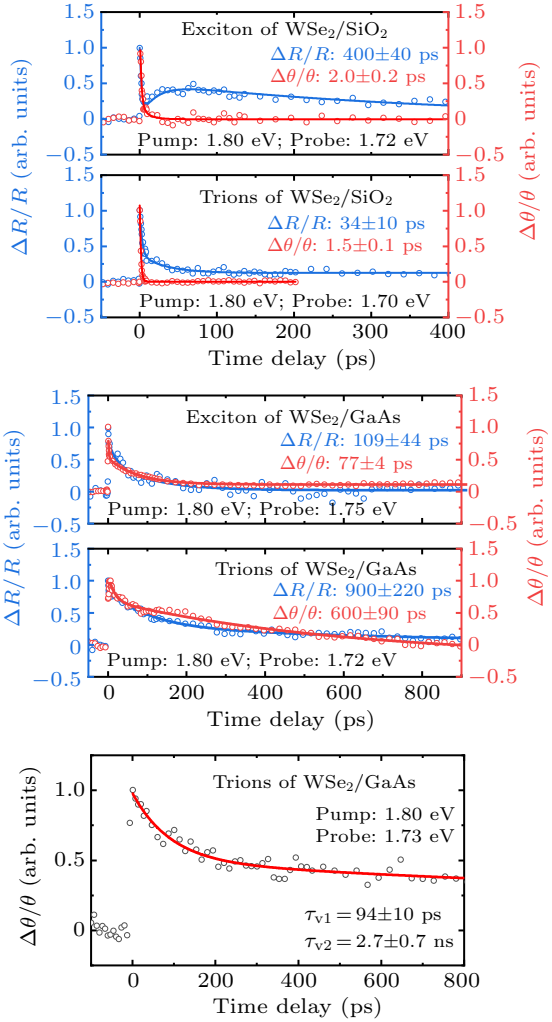



**Fig. 4.** The TRR and TRKR results measured with pump photon energy of 1.80 eV, and probe photon energy tuned to be resonant with the exciton and trions for (a) $WSe_2/SiO_2$ and (b) $WSe_2$/GaAs. Lifetimes noted in (a), (b) are long-lived components extracted from the bi-exponential fittings. It is seen that the valley polarization of trions in $WSe_2$/GaAs survives two orders of magnitude longer than that in $WSe_2/SiO_2$. (c) TRKR results under pumping at 1.80 eV and fine tuning probe at 1.73 eV for the trions in $WSe_2$/GaAs.

To further understand the charge transfer process in $WSe_2$/GaAs heterostructure, we then investigate the carrier dynamics of GaAs for both the heterostructure and the GaAs wafer, by fixing the probe photon energy in resonance with the bandgap of GaAs (1.514 eV) at 10 K, and tuning the pump photon energy at 1.57 eV and 1.80 eV for both $WSe_2$/GaAs and GaAs wafer. The results presented in Fig. 5(a) indicate that, when pumping near the GaAs bandgap, the GaAs reference wafer showed decreased reflectivity around zero time delay, followed by a rapid increase, and then decreased again. This phenomenon has been observed previously and was attributed to the competition between the band-filling effect (enhanced reflectivity) and the bandgap renormalization effect (reduced reflectivity).[53] Bandgap renormalization $\Delta E_g$ is written as[54]

$$\Delta E_{\mathrm{g}} = -\sum_{q\neq 0} V_{\mathrm{s}}(q)[f_{\mathrm{e}}(q)+f_{\mathrm{h}}(q)] - \sum_{q\neq 0}[V_{\mathrm{s}}(q)-V(q)], \quad (1)$$

where $V(q)$ and $V_{\mathrm{s}}(q)$ are the Fourier transforms of the unscreened and screened Coulomb potentials, respectively; $q$ represents the electron momentum; $f_{\mathrm{e}}(q)$ and $f_{\mathrm{h}}(q)$ are the electron and hole occupation probabilities of states. $|\Delta E_{\mathrm{g}}|$ represents the degree of bandgap renormalization. Under optical excitation with pumping photon energy of 1.57 eV for $WSe_2$/GaAs and GaAs reference wafer, Fig. 5(a) shows a decreased bandgap renormalization effect ($|\Delta E_{\mathrm{g}}|$) in the heterostructure compared with that of GaAs reference sample, indicating a dominant decrease of $f_{\mathrm{h}}(q)$ arising from the hole transfer from GaAs to $WSe_2$, since only optically excited holes in GaAs can transfer to $WSe_2$ at near-resonant excitation of GaAs, as illustrated in Fig. 5(c). However, under pumping at 1.80 eV where both $WSe_2$ and GaAs can be simultaneously excited, $|\Delta E_{\mathrm{g}}|$ of the heterostructure surpasses that of the reference GaAs as seen in Fig. 5(b). This result suggests that electrons transfer more efficiently from $WSe_2$ to GaAs than holes from GaAs to $WSe_2$, since the conduction band offset (0.6 eV) is larger than that of the valence band (0.1 eV) in $WSe_2$/GaAs heterostructure.[30]

In addition, under near-resonant excitation of GaAs at 1.57 eV presented in Fig. 5(a), long carrier lifetimes of ~1.6 ns for $WSe_2$/GaAs heterostructure and ~ 1.2 ns for GaAs reference sample were evaluated. While for the off-resonant excitation at 1.80 eV as shown in Fig. 5(b), the carrier lifetime of GaAs was reduced to ~ 0.67 ns for GaAs reference wafer, which was attributed to the strengthened momentum scattering under above-bandgap excitation. However, under the off-resonant excitation, it is noticed that the carrier lifetime of GaAs can be extended to ~ 2.0 ns in $WSe_2$/GaAs heterostructure, which is longer than that of near-resonant excitation case and is nearly three times longer than that of GaAs reference sample. The prolonged carrier lifetime of GaAs under off-resonant excitation at 1.80 eV, at which both $WSe_2$ and GaAs can be optically excited, was attributed to the enhanced charge transfer between $WSe_2$ and GaAs driven by optical excitation. Since the electron–hole recombination can be further suppressed owing to the reduced available hole states at GaAs band edges, as a result of interfacial hole transfer from GaAs to $WSe_2$. The results also imply that the carrier relaxation in

GaAs for $WSe_2$/GaAs is governed by the electrons experiencing non-radiative scattering instead of electron–hole recombination. The long lifetime up to nanosecond for both the exciton of $WSe_2$ and carriers of GaAs in $WSe_2$/GaAs heterostructure, is favorable for designing the related high-performance opto-electronics.

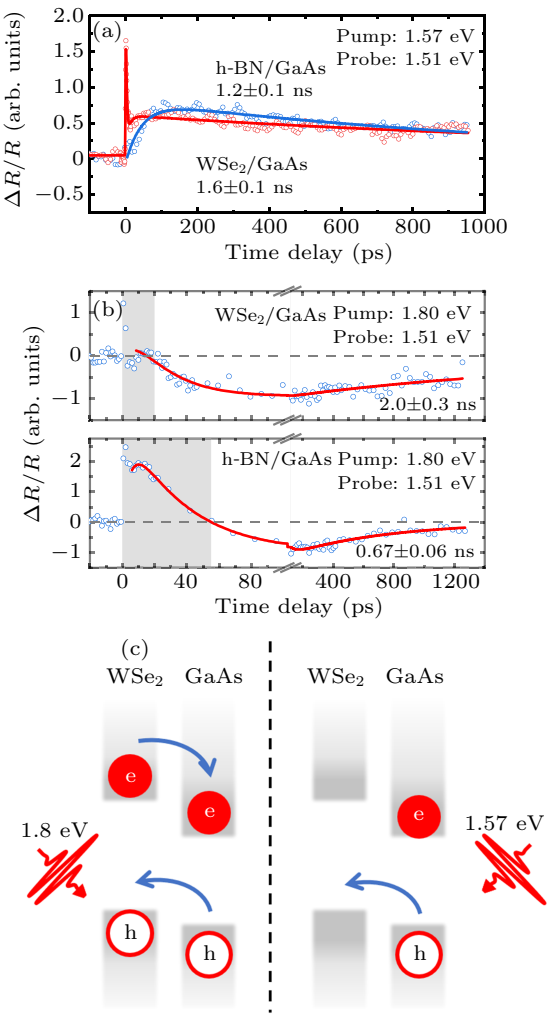



**Fig. 5.** The $\Delta R/R$ measurements at 10 K for the carrier dynamics of GaAs in both the $WSe_2$/GaAs heterostructure and GaAs wafer. Here, the probe photon energy was fixed to be in resonance with the bandgap of GaAs at 10 K (1.514 eV). (a) The $\Delta R/R$ results measured at pump photon energy of 1.57 eV, at which only GaAs can be optically excited. The excited holes in GaAs transfer to $WSe_2$, resulting in the reduced band renormalization of GaAs. (b) The $\Delta R/R$ results measured at pump photon energy of 1.80 eV. Both GaAs and $WSe_2$ can be optically excited, so that electrons in $WSe_2$ can participate in the transfer process, giving rise to significant band renormalization of GaAs. (c) Schematic diagram of charge transfer process under different excitation conditions.

## 4. Conclusion and perspectives

In summary, the exciton and valley depolarization dynamics in $WSe_2$/GaAs heterostructure have been systematically investigated by varying pump and probe photon energies. It is observed that the exciton of $WSe_2$ and carriers of GaAs in $WSe_2$/GaAs heterostructure have prolonged lifetimes up to nanosecond timescale, which are longer than those of the monolayer $WSe_2$ and GaAs reference samples. The charge transfer is discussed to play a significant role in our experimental findings. Especially, the resident electrons accumulated at the interface by the charge-transfer induced interfacial electric field, facilitate the formation of the long-lived polarized trions that possess a high polarization degree of $\sim 70\%$ and long valley lifetime of $\sim 2.7$ ns. This work reveals that the $WSe_2$/GaAs heterostructure has great potential for designing high-performance optoelectronic and spintronic devices, with further optimal design of doping and controllable charge transfer via an external gate.

## Acknowledgements

This work was funded by the National Key Research and Development Program of China (Grant No. 2022YFA1405100) and the Strategic Priority Research Program of the Chinese Academy of Sciences (Grant No. XDB43000000).

## References

[1] Sierra J F, Fabian J, Kawakami R K, Roche S and Valenzuela S O 2021 *Nat. Nanotechnol.* **16** 856
[2] Liu Y, Huang Y and Duan X 2019 *Nature* **567** 323
[3] Jiang Y, Chen S, Zheng W, Zheng B and Pan A 2021 *Light Sci. Appl.* **10** 72
[4] Manzeli S, Ovchinnikov D, Pasquier D, Yazyev O V and Kis A 2017 *Nat. Rev. Mater.* **2** 1
[5] Wang G, Chernikov A, Glazov M M, Heinz T F, Marie X, Amand T and Urbaszek B 2018 *Rev. Mod. Phys.* **90** 021001
[6] Xiao D, Liu G B, Feng W, Xu X and Yao W 2012 *Phys. Rev. Lett.* **108** 196802
[7] Le D, Barinov A, Preciado E, Isarraraz M, Tanabe I, Komesu T, Troha C, Bartels L, Rahman T S and Dowben P A 2015 *J. Phys.: Condens. Matter* **27** 182201
[8] Volmer F, Pissinger S, Ersfeld M, Kuhlen S, Stampfer C and Beschoten B 2017 *Phys. Rev. B* **95** 235408
[9] Song X, Xie S, Kang K, Park J and Sih V 2016 *Nano Lett.* **16** 5010
[10] Wang G, Bouet L, Lagarde D, Vidal M, Balocchi A, Amand T, Marie X and Urbaszek B 2014 *Phys. Rev. B* **90** 075413
[11] Somvanshi D and Jit S 2020 *Micro and Nano Technologies* Ed. Jit S and Das S (Elsevier) p. 125
[12] Lyons T P, Gillard D, Molina-Sánchez A, Misra A, Withers F, Keatley P S, Kozikov A, Taniguchi T, Watanabe K, Novoselov K S, Fernández-Rossier J and Tartakovskii A I 2020 *Nat. Commun.* **11** 6021
[13] Zhong Y, Yue S, Liang J, Yuan L, Xia Y, Tian Y, Zheng Y, Zhang Y, Du W, Li D, Chen S, Pan A and Liu X 2025 *Nano Lett.* **25** 5274
[14] Chen H, Wen X, Zhang J, Wu T, Gong Y, Zhang X, Yuan J, Yi C, Lou J, Ajayan P M, Zhuang W, Zhang G and Zheng J 2016 *Nat. Commun.* **7** 12512
[15] Hong X, Kim J, Shi S-F, Zhang Y, Jin C, Sun Y, Tongay S, Wu J, Zhang Y and Wang F 2014 *Nat. Nanotechnol.* **9** 682
[16] Liu H, Zhang Z, Zhang C, Li X, Zhang C, Xu F, Wu Y, Wu Z and Kang J 2024 *Nano Lett.* **24** 1851
[17] Hwang A, Park M, Park Y, Shim Y, Youn S, Lee C H, Jeong H B, Jeong H Y, Chang J, Lee K, Yoo G and Heo J 2021 *Sci. Adv.* **7** eabj2521
[18] Sharma I and Mehta B R 2017 *Appl. Phys. Lett.* **110** 061602
[19] Li K, Wang W, Li J, Jiang W, Feng M and He Y 2020 *Photon. Res.* **8** 1368
[20] Xu Z, Lin S, Li X, Zhang S, Wu Z, Xu W, Lu Y and Xu S 2016 *Nano Energy* **23** 89
[21] Jin C, Ma E Y, Karni O, Regan E C, Wang F and Heinz T F 2018 *Nat. Nanotechnol.* **13** 994
[22] Ciarrocchi A, Tagarelli F, Avsar A and Kis A 2022 *Nat. Rev. Mater.* **7** 449

[23] Ajayan J, Nirmal D, Mohankumar P, Kuriyan D, Fletcher A S A, Arivazhagan L and Kumar B S 2019 *Microelectron. J.* **92** 104604

[24] Kikkawa J M and Awschalom D D 1998 *Phys. Rev. Lett.* **80** 4313

[25] Dzhioev R I, Kavokin K V, Korenev V L, Lazarev M V, Meltser B Ya, Stepanova M N, Zakharchenya B P, Gammon D and Katzer D S 2002 *Phys. Rev. B* **66** 245204

[26] Uemura T, Akiho T, Ebina Y and Yamamoto M 2015 *Phys. Rev. B* **91** 140410

[27] Ebina Y, Akiho T, Liu H, Yamamoto M and Uemura T 2014 *Appl. Phys. Lett.* **104** 172405

[28] Manna S, Huang H, da Silvaa S F C, Schimpfa C, Rotab M B, Lehnera B, Reindla M, Trottab R and Rastelli A 2020 *Appl. Surf. Sci.* **532** 147360

[29] Rojas-Lopez R R, Hendriks F, van der Wal C H, Guimarães P S S and Guimarães M H D 2024 *Appl. Phys. Lett.* **125** 132104

[30] Pierucci D, Mahmoudi A, Silly M, Bisti F, Oehler F, Patriarche G, Bonell F, Marty A, Vergnaud C, Jamet M, Boukari H, Lhuillier E, Pala M and Ouerghi A 2022 *Nanoscale* **14** 5859

[31] Yan T, Ye J, Qiao X, Tan P and Zhang X 2017 *Phys. Chem. Chem. Phys.* **19** 3176

[32] Li Z, Wang T, Lu Z, Jin C, Chen Y, Meng Y, Lian Z, Taniguchi T, Watanabe K, Zhang S, Smirnov D and Shi S F 2018 *Nat. Commun.* **9** 3719

[33] Jones A M, Yu H, Ghimire N J, Wu S, Aivazian G, Ross J S, Zhao B, Yan J, Mandrus D G, Xiao D, Yao W and Xu X 2013 *Nat. Nanotechnol.* **8** 634

[34] Li J, Goryca M, Yumigeta K, Li H, Tongay S and Crooker S A 2021 *Phys. Rev. Mater.* **5** 044001

[35] Cadiz F, Courtade E, Robert C, Wang G, Shen Y, Cai H, Taniguchi T, Watanabe K, Carrere H, Lagarde D, Manca M, Amand T, Renucci P, Tongay S, Marie X and Urbaszek B 2017 *Phys. Rev. X* **7** 021026

[36] Borghardt S, Tu J S, Winkler F, Schubert J, Zander W, Leosson K and KardynałB E 2017 *Phys. Rev. Mater.* **1** 054001

[37] Raja A, Waldecker L, Zipfel J, Cho Y, Brem S, Ziegler J D, Kulig M, Taniguchi T, Watanabe K, Malic E, Heinz T F, Berkelbach T C and Chernikov A 2019 *Nat. Nanotechnol.* **14** 832

[38] Yan T, Qiao X, Liu X, Tan P and Zhang X 2014 *Appl. Phys. Lett.* **105** 101901

[39] Moody G, Schaibley J and Xu X 2016 *J. Opt. Soc. Am. B* **33** C39

[40] Cadiz F, Robert C, Courtade E, Manca M, Martinelli L, Taniguchi T, Watanabe K, Amand T, Rowe A C H, Paget D, Urbaszek B and Marie X 2018 *Appl. Phys. Lett.* **112** 152106

[41] Li Y, Shi J, Mi Y, Sui X, Xu H and Liu X 2019 *J. Mater. Chem. C* **7** 4304

[42] Wang Q, Ge S, Li X, Qiu J, Ji Y, Feng J and Sun D 2013 *ACS Nano* **7** 11087

[43] Wang H, Zhang C and Rana F 2015 *Nano Lett.* **15** 339

[44] Sun D, Lai J W, Ma J C, Wang Q S and Liu J 2017 *Chin. Phys. B* **26** 037801

[45] Ye J, Niu B, Li Y, Li T and Zhang X 2017 *Appl. Phys. Lett.* **111** 152106

[46] Zhu C R, Zhang K, Glazov M, Urbaszek B, Amand T, Ji Z W, Liu B L and Marie X 2014 *Phys. Rev. B* **90** 161302

[47] Hu S, Ye J, Liu R and Zhang X 2022 *J. Semicond.* **43** 082001

[48] Yu T and Wu M W 2014 *Phys. Rev. B* **89** 205303

[49] Glazov M M, Ivchenko E L, Wang G, Amand T, Marie X, Urbaszek B and Liu B L 2015 *Phys. Status Solidi B* **252** 2349

[50] Hsu W T, Chen Y L, Chen C H, Liu P S, Hou T H, Li L J and Chang W H 2015 *Nat. Commun.* **6** 8963

[51] Yang L, Sinitsyn N A, Chen W, Yuan J, Zhang J, Lou J and Crooker S A 2015 *Nat. Phys.* **11** 830

[52] Cheng C, Sun J T, Chen X R, Fu H X and Meng S 2016 *Nanoscale* **8** 17854

[53] Teng L H, Wang X and Lai T S 2011 *Acta Phys. Sin.* **60** 047201 (in Chinese)

[54] Chernikov A, Ruppert C, Hill H M, Rigosi A F and Heinz T F 2015 *Nat. Photonics* **9** 466